Performance comparison of HDG and classical DG method for the simulation of seismic wave propagation in harmonic domain

Marie Bonnasse-Gahot, Stéphane Lanteri, Julien Diaz, Henri Calandra

Marie BONNASSE-GAHOT
Advisors :
Stéphane LANTERI,
Equipe-Projet INRIA Nachos
Julien DIAZ,
Equipe-Projet INRIA Magique-3D
& Henri CALANDRA
CSTJF Total

Mail : marie.bonnasse-gahot@inria.fr
Equipe-Projet Magique-3D
INRIA - Bordeaux Sud-Ouest
Université de Nice-Sophia-Antipolis
Inria-Total action Depth Imaging Partnership (DIP)

Performance comparison of HDG and classical DG method for the simulation of seismic wave propagation in harmonic domain

Motivation and context

As the drilling is expensive, the petroleum industry is interested by methods able to produce images of the intern sturctures of the Earth before the drilling.
Seismic imaging can be processed in time-domain or in harmonic-domain.The imaging condition is easier to implement in frequency domain, but solving the Helmholtz equations in 3D is almost impossible due to a huge computationnal cost, even with the help of High Performance Computing. We then have to develop less expensive methods.
One of seismic imaging methods in harmonic-domain is the full wave inversion (FWI), giving us quantitative high resolution images of the subsurface. It defines an inverse problem and needs of the full wave form (FWF).
To obtain this FWF we need to solve the forward problem : the Helmholtz equations. We are interested in reducing the size of the linear system that we have to solve.

Seismic survey on earth

Seismic survey on sea

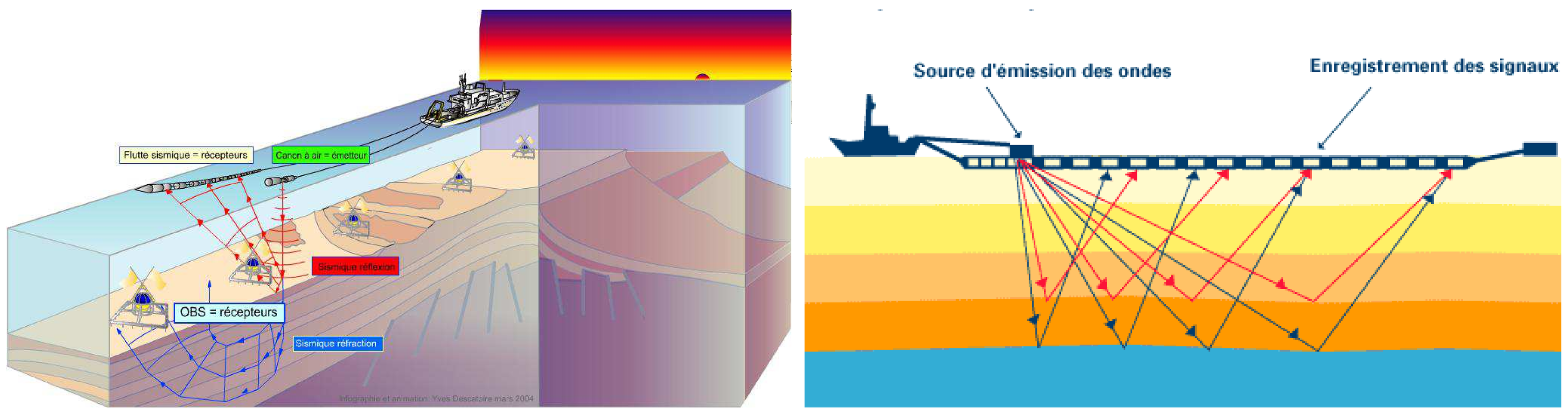

Acquisition methods

2D Helmholtz isotropic elastic equations

Equations

For $\mathbf{x} = (x, z) \in \Omega \subset \mathbb{R}^2$:

$$\begin{cases} i\omega\rho(\mathbf{x})\mathbf{v}(\mathbf{x}) = \nabla \cdot \underline{\sigma}(\mathbf{x}) + f(\mathbf{x}) & \text{in } \Omega \\ i\omega\underline{\sigma}(\mathbf{x}) = \underline{\underline{C}}(\mathbf{x})\ \underline{\epsilon}(\mathbf{v}(\mathbf{x})) & \text{in } \Omega \end{cases}$$

with : $\rho(\mathbf{x}) > 0$ the medium density ; $\mathbf{v}(\mathbf{x}) = (\ v_x(\mathbf{x}),\ v_z(\mathbf{x})\ )^T$, the velocity vector ; $\underline{\epsilon}$ the strain tensor with $\epsilon_{ij} = \frac{1}{2}\left(\frac{\partial v_i}{\partial j} + \frac{\partial v_j}{\partial i}\right)$, $i, j = x, z$; $\underline{\sigma}$ the stress tensor, in the isotropic case $\sigma_{ij} = \lambda\delta_{ij}tr(\underline{\epsilon}) + 2\mu\epsilon_{ij}$, $i, j = x, z$; $\underline{\underline{C}}$ the stiffness tensor depending on λ and μ the Lamé's coefficients, and $f(\mathbf{x})$ volumic forces.

These two equations can be rewrite as vectorial form :

$$i\omega\mathbf{W} + \mathbf{A_x}\frac{\partial \mathbf{W}}{\partial x} + \mathbf{A_z}\frac{\partial \mathbf{W}}{\partial z} = 0$$

where $\mathbf{W} = (v_x, v_z, \sigma_{xx}, \sigma_{zz}, \sigma_{xz})^{\mathrm{T}}$ and $\mathbf{A_x}$ and $\mathbf{A_z}$ are matrices containing physical parameters.

Modelling of the problem : Discontinuous Galerkin (DG) formulations

Classical DG method VS HDG method

The main difference between classical DG methods and the hybridizable DG method (see [1] for more details) is the number of degrees of freedom (dof). In classical DGM, basis functions are continuous over an element but discontinuous at its interfaces, so the dof only belong to one element. In HDGM, basis functions are continuous over a face and discontinuous at its boundaries.

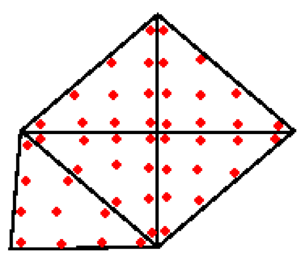

Degrees of freedom of DGM

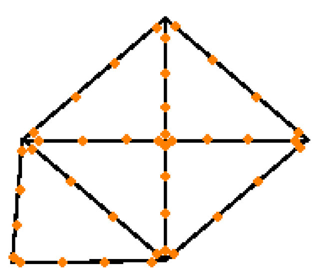

Degrees of freedom of HDGM

Local Upwind fluxes DG formulation

$$\int_K i\omega\mathbf{W}^K\varphi - \int_K \mathbf{A}_x\mathbf{W}^K\frac{\partial\varphi}{\partial x} - \int_K \mathbf{A}_z\mathbf{W}^K\frac{\partial\varphi}{\partial z} + \int_F (\mathbf{D_n}\mathbf{W})|_F = 0$$

where $\mathbf{D_n} = n_x\mathbf{A}_x + n_z\mathbf{A}_z$. On a face F, for the upwind scheme, we express the flux term on the same way that it is expressed in [4] :

$$(\mathbf{D_n}\mathbf{Q})|_F = \left(\mathbf{D}_\mathbf{n}^K\right)^+\mathbf{Q}^K + \left(\mathbf{D}_\mathbf{n}^{K'}\right)^-\mathbf{Q}^{K'}$$

where $\mathbf{D}_\mathbf{n}^+ = \mathbf{R_n}\Gamma^+(\mathbf{R_n})^{-1}$ and $\mathbf{D}_\mathbf{n}^- = \mathbf{R_n}\Gamma^-(\mathbf{R_n})^{-1}$. Γ^+ is the matrix containing the positive eigenvalues of $\mathbf{D_n}$ and Γ^- the negative eigenvalues of $\mathbf{D_n}$. $\mathbf{R_n}$ is the matrix containing the corresponding eigenvectors.

We obtain the following upwind fluxes DG formulation

$$\int_K i\omega\mathbf{W}^K\varphi - \int_K \mathbf{A}_x^K\mathbf{W}^K\frac{\partial\varphi}{\partial x} - \int_K \mathbf{A}_z^K\mathbf{W}^K\frac{\partial\varphi}{\partial z} + \sum_F\int_F\left[\left(\mathbf{D}_\mathbf{n}^K\right)^+\mathbf{W}^K + \left(\mathbf{D}_\mathbf{n}^{K'}\right)^-\mathbf{W}^{K'}\right]\varphi = 0$$

Local Hybridizable DG formulation

$$\begin{cases} \int_K i\omega\rho^K\mathbf{v}^K\cdot\mathbf{w} + \int_K \underline{\sigma}^K : \nabla\mathbf{w} - \int_{\partial K}\widehat{\underline{\sigma}}^{\partial K}\cdot\mathbf{n}\cdot\mathbf{w} = 0 \\ \int_K i\omega\underline{\sigma}^K : \underline{\xi} + \int_K \mathbf{v}^K\cdot\nabla\cdot\left(\underline{\underline{C}}^K\underline{\xi}\right) - \int_{\partial K}\widehat{\mathbf{v}}^{\partial K}\cdot\underline{\underline{C}}^K\underline{\xi}\cdot\mathbf{n} = 0 \end{cases}$$

We define $\widehat{\mathbf{v}}^F = \lambda^F, \forall F$ and $\widehat{\underline{\sigma}}^{\partial K}\cdot\mathbf{n} = \underline{\sigma}^K\cdot\mathbf{n} - \tau\mathbf{I}\left(\mathbf{v}^K - \lambda^{\partial K}\right)$ on ∂K according to the definitions giving in [3]. τ is the stabilization parameter ($\tau > 0$). With this, we obtain the local HDG formulation :

$$\begin{cases} \int_K i\omega\rho^K\mathbf{v}^K\cdot\mathbf{w} - \int_K\left(\nabla\cdot\underline{\sigma}^K\right)\cdot\mathbf{w} + \int_{\partial K}\tau\mathbf{I}\left(\mathbf{v}^K - \lambda^{\partial K}\right)\cdot\mathbf{w} = 0 \\ \int_K i\omega\underline{\sigma}^K : \underline{\xi} + \int_K \mathbf{v}^K\cdot\nabla\cdot\left(\underline{\underline{C}}^K\underline{\xi}\right) - \int_{\partial K}\lambda^{\partial K}\cdot\underline{\underline{C}}_K\underline{\xi}\cdot\mathbf{n} = 0 \end{cases}$$

Finally, in order to determine λ, we need to introduce a third equation, which more renders the numerical trace conservative, the so-called transmission condition traduced by :

$$\int_F [\![\widehat{\underline{\sigma}}^K\cdot\mathbf{n}]\!]\cdot\eta = 0$$

Numerical Results

Disk-shaped scatterer problem

On this test-case, if we normalize the computational performances of the HDG method and if we look at the ratio with two others classical DG methods, we can see that we are at least 3 times better with order 2 in terms of CPU Time and 2 times better in memory. If we increase the interpolation order, we remark that we are still at least 3 times better in CPU time but in memory we are now at least 5 times better.

Elements	Order	CPU Time			Memory		
		HDG	UDG	IPDG	HDG	UDG	IPDG
1200	2	1	3.7	3.4	1	8.4	2.2
5100	2	1	5.0	4.0	1	8.4	2.3
21000	2	1	6.8	4.1	1	9.0	2.6
1200	3	1	3.1	4.0	1	9.2	3.3
5100	3	1	5.1	4.7	1	10.3	3.6
21000	3	1	7.2	5.7	1	11.0	4.0
1200	4	1	2.7	4.0	1	10.4	5.0
5100	4	1	3.8	5.0	1	10.5	5.3
21000	4	1	5.7	6.6	1	10.8	5.9

Marmousi test-case

Computational domain Ω composed of 235000 triangles

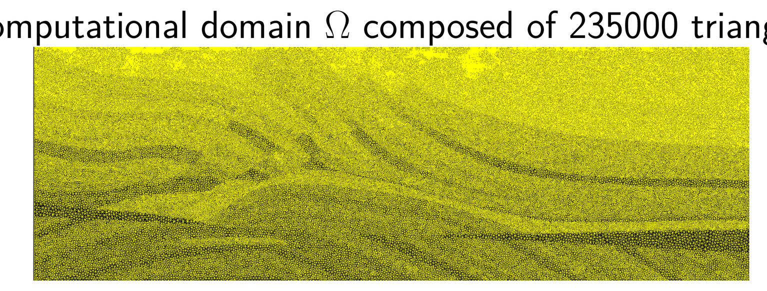

Parallel results with the HDG-P2 scheme

	CPU Time construction (s)	CPU Time resolution. (s)	Maximum Memory (MB)
sequential	67	133	9927
2 proc. (2/1)	32	93	5892
4 proc. (2/2)	15	56	3340
8 proc. (4/2)	8	38	2092
16 proc. (4/4)	4	39	3695
32 proc. (4/8)	2	21	1312
64 proc. (8/8)	1	19	893

Conclusions and Perspectives

With HDG scheme we do not loose the convergence order $(p+1)$ that we have with classical DG methods. Moreover on a same mesh the HDG formulation is more competitive in terms of memory and computational time than the upwind flux DG formulation and the IPDG method.
Now we are interested to develop 3D HDG formulation for the Helmholtz equations and to study a specific solution strategy for the HDG linear system.

References

[1] B. Cockburn, J. Gopalakrishnan, R. Lazarov. Unified hybridization of discontinuous Galerkin, mixed and continuous Galerkin methods for second order elliptic problems. *SIAM Journal on Numerical Analysis*, Vol. **47**, 2009.
[2] S. Lanteri, L. Li, R. Perrussel. Numerical investigation of a high order hybridizable discontinuous Galerkin method for 2d time-harmonic Maxwell's equations. *COMPEL*, Vol. **32**, 2013.
[3] N.C. Nguyen, J. Peraire, B. Cockburn. High-order implicit hybridizable discontinuous Galerkin methods for acoustics and elastodynamics. *J. of Comput. Physics*, Vol. **230**, 2011.
[4] M. El Bouajaji, S. Lanteri. High order discontinuous Galerkin method for the solution of 2D time-harmonic Maxwell's equations. *Applied Mathematics and Computation*, Vol. **219**, 7241–7251, 2013.